Article:
Su, J., Li, K. and Xing, C. (2023) Plug-and-Play of Grid-Forming Units in DC Microgrids Assisted with Power Buffers. IEEE Transactions on Smart Grid. ISSN: 1949-3053

https://doi.org/10.1109/tsg.2023.3296799

Plug-and-Play of Grid-Forming Units in DC Microgrids Assisted with Power Buffers

Jialei SU, Kang LI, *Senior member, IEEE*, Chen XING

***Abstract*—Grid-forming units (GFUs) are fundamental devices in DC microgrids for DC bus voltage regulation. Droop control is widely used for GFU control due to its Plug-and-Play feature. However, it may fail to meet some desired DC microgrid control features and performances, such as zero steady-state DC bus voltage deviation, high system inertia, and fast DC bus voltage regulation. To achieve these desired control performances, some advanced control strategies have been proposed, but the introduction of time-dependent terms or the centralized controller in these control strategies leads to the loss of the key Plug-and-Play feature for GFUs. To maintain the Plug-and-Play feature of GFUs while meeting the desired microgrid control features and performances, this paper proposes a power buffer based control framework. The power buffer is a new device combing a capacitor and a bidirectional DC-DC converter as an interface between GFUs and the DC bus. It enables the development of a novel decoupled control strategy where GFUs are regulated by the droop control while advanced control strategies are applied to the power buffer. Thus, the Plug-and-Play feature of GFUs is maintained, while specific DC microgrid performances are also achieved simultaneously. Supported by this power buffer based control framework, GFUs can be plugged in/out DC microgrids seamlessly at any time without introducing DC bus voltage fluctuations. This allows GFUs, especially mobile GFUs, to achieve high DC bus voltage regulation performance. The hardware-in-loop (HIL) test and real circuit experimental results demonstrate its efficacy.**

***Index Terms*—Multiple GFUs, Power buffer, Droop control, Plug-and-Play, DC microgrids.**

I. Introduction

THE past last few years have witnessed a rapid development of distributed energy resources (DERs) such as renewable energy sources (RESs) and energy storage systems (ESSs) to support the power system decarbonization [1]. The concept of microgrid has emerged as an effective way to coordinate the RESs and the loads [2]. Among the two popular types of microgrids, namely the AC microgrids and DC microgrids, the latter is becoming more attractive as many existing sources and loads are DC-based, like photovoltaic (PV) panels, battery energy storage systems (BESSs), and electric vehicles (EVs). Compared with its AC counterpart, DC microgrids have some distinctive features, such as no frequency/reactive power control, and no need for harmonics cancellation [3].

RESs like PV panels and wind turbines (WTs), usually work at maximum power point tracking (MPPT) to fully explore renewable energy such that their output power matches the weather conditions, like solar irradiance and wind speed [4]. Considering the stochastic nature of RESs and unpredictable variation of the loads, grid-forming units (GFUs) are introduced in DC microgrids to regulate the DC bus voltage and compensate the power mismatch between RESs and loads [5], [6]. Generally speaking, GFUs should allow bidirectional power flow. Utility grid, external DC microgrids, external AC microgrids, and ESSs can all work as GFUs [7], [8] to support a specific DC microgrid with the assistance of power electronic devices and associated control strategies, and different types of ESSs can be used in DC microgrids, like batteries, supercapacitors (SCs), fuel cells, etc [9].

The control objectives of these GFUs include DC bus voltage regulation and power-sharing among them. The droop control works in a decentralized way and is widely used in GFUs control. It linearly decreases the output voltage with output current increases, in this way, the aforementioned two control objectives are achieved simultaneously with the droop control [10], [11]. The droop control can be implemented either in the current mode or the voltage mode, and the output voltage is used as feedback to determine output current in the current mode, while the output current is used to determine output voltage in the voltage mode [12].

Although the droop controlled GFUs work in a decentralized way and have Plug-and-Play functionality, some specific and desirable DC microgrid performances can not be achieved with droop control, e.g., zero steady-state voltage deviation between the nominal and measured DC bus voltage, requirement of high system inertia, and fast DC bus voltage regulation. To meet these requirements, some advanced control strategies are introduced. For example, secondary control is proposed to eliminate the deviation between nominal voltage and measured DC bus voltage due to the droop control, where the measured DC bus voltage is used as feedback to generate a secondary control signal for output voltage modification [13], [14]. Xing et al proposed a distributed secondary control for voltage restoration and current-sharing in DC microgrids, where the communication link between GFUs are needed [15], [16]. DC microgrids are often low-inertia grids dominated by power electronics, the system stability is a serious issue for these low-inertia microgrids. To increase the system inertia, some virtual inertia control (VIC) strategies are used. For example, a VIC strategy for DC microgrids is proposed in [17] through bidirectional converters analogous to the virtual synchronous machine (VSM). A bidirectional virtual inertia support strategy is proposed in [18] for hybrid microgrids, where the inertia is delivered to both AC and DC subgrids via the control of a bidirectional interlinking converter. In [17], [18], the rate-of-change-of-voltage (RoCoV) is reduced and system stability is increased with the introduced virtual inertia.

Besides secondary control and VIC, other advanced control strategies are also proposed to achieve an even bet-

ter DC microgrid performance, e.g., model predictive control (MPC), fuzzy logic control (FLC), and artificial-neural-network (ANN)-based control. Shan et al proposed an MPC for BESS in [19], where BESS collects the information of RESs and loads, fast DC bus voltage regulation is achieved and power mismatch between RESs and loads is compensated. Two independent fuzzy logic controllers (one for BESS and one for utility grid) are proposed in [20] to maintain the DC bus voltage and BESS state-of-charge (SoC) within proper thresholds. ANN-based controllers are proposed in [21] for PV, WT and BESS to reduce the number of sensors, where the load demands are satisfied with a rapid response, while fewer oscillations and greater reliability tolerance are achieved.

In the most aforementioned advanced control strategies, the Plug-and-Play feature of GFUs are lost due to different reasons. In the secondary control and VIC, the time-dependent terms like 'integrator' are used in the controller design, which introduces the time-dependent power-sharing functionality among GFUs. In other words, the controller performance is dependent on the connection time of GFUs. Therefore, the Plug-and-Play functionality of GFUs is lost for secondary control and VIC. The MPC/FLC/ANN-based control usually work in a centralized way, where the information of all other DERs needs to be collected and the control strategies need to be redesigned when new devices are introduced, thus the Plug-and-Play functionality of GFUs is also lost. However, it is a future trend that GFUs have the Plug-and-Play feature when they are connected to the DC microgrids [22]. The system scalability and reliability are increased for microgrids with the Plug-and-Play feature [23]. Li et al proposed a module-based Plug-and-Play DC microgrids to support rural electrification. It provides a bottom-up approach to form a microgrid with multilayer expandability and Plug-and-Play feature [24]. A decentralized PV–BESS coordination control method for Plug-and-Play DC microgrid is also proposed in [25].

Albeit some of the control strategies, e.g., in some papers like [15], [16] also have the Plug-and-Play feature, they require the communication links between GFUs. Unlike droop controlled GFUs, the flexibility of GFUs (especially for mobile GFUs like EVs and DC ship microgrids) are inevitably reduced due to the requirement for the communication links. Firstly, the communication links between the new plug in GFUs and other GFUs need to be added when the former are connected to the DC microgrids. Secondly, the communication links for GFUs in distributed control strategies are usually modeled as a directed graph, which lose its controllability and observability as some GFUs are plugged out, hence imposing major negative impacts on the DC microgrid performances. Recently, DC microgrids with dynamic topology and mobile GFUs are becoming increasing attractive in recent years [26], as these mobile GFUs can be re-located in response to changing microgrid conditions, e.g., support overloaded microgrids and then move to other places once the demand drops in these overloaded microgrids [27]. Further, mobile GFUs can also provide power support during emergency conditions and for post-disaster restoration [28], [29]. In these application scenarios, droop controlled mobile GFUs will offer more flexibility compared to other control strategies.

In summary, the Plug-and-Play functionality of GFUs and their flexibility are maintained if the droop control is applied, however, it may not achieve other desired DC microgrid performances. Better DC microgrid performances can be achieved by advanced control strategies but the Plug-and-Play functionality of GFUs is lost. To address this dilemma and one of the major challenges in the controller design of DC microgrids, a power buffer based control framework is proposed in this paper to bridge the gap and it retains the advantages of both the droop control and advanced control strategies. The power buffer concept was originally proposed in the previous work for power allocation between batteries and SCs in dynamically forming multiple hybrid ESSs [30]. This paper incorporates the power buffer device into the DC microgrids to address one of the most challenging control issues, namely achieving desired control performances which usually are reliant on advanced control strategies, while maintaining the Plug-and-Play features of GFUs which usually be maintained by simple droop control. In essence, the power buffer, as an interface between GFUs and the DC bus, has provided an extra dimension of control freedom, where GFUs are droop controlled, hence maintaining the Plug-and-Play functionality. While the advanced control strategy is applied to the power buffer to achieve DC microgrid performances. The main contributions of this paper are summarized as follows.

1) A power buffer based control framework is proposed for DC microgrids, where GFUs are regulated by the droop control while the advanced control strategies are applied to the power buffer. This controller design retains the the Plug-and-Play feature of GFUs while simultaneously achieving the desired DC microgrid control performances.

2) The small-signal analysis is conducted to validate the stability of the proposed control framework, further revealing that the controller parameters and device parameters for both GFUs and power buffer converters can be designed separately.

3) Within this control framework, large droop coefficients can be designed to ensure accurate power-sharing among GFUs. Given that no loads/RESs are connected to the power buffer capacitor, a large voltage drop caused by large droop coefficients is acceptable.

The remainder of this paper is organized as follows. Section II briefly introduces the configuration of DC microgrids. In Section III, different control strategies for GFUs and their Plug-and-Play feature are discussed. The proposed power buffer based control framework and small-signal stability analysis are presented in Section IV. The results of hardware-in-loop (HIL) test results of the proposed strategy are given in Section V. The real circuit experiment is presented in the Section VI. Finally, Section VII concludes the paper.

II. Configuration of DC Microgrids

The configuration of a typical DC microgrid is illustrated in Fig.1. RESs such as WTs and PV panels are connected and import power to DC microgrids, and they usually work at MPPT to fully utilize available renewable energy. Besides RESs, the DC loads and AC loads are also connected to DC bus, they absorb power from DC bus. To deal with the intermittent and

stochastic nature of RESs and unpredictable variation of loads, GFUs are introduced to provide bidirectional power support to DC microgrids. All RESs, loads, and GFUs are connected to a common DC bus. To present the power mismatch between RES and loads, the equivalent load current I_0 is defined as

$$I_0 = I_{dc,load} + I_{ac,load} - I_{pv} - I_{wt} \tag{1}$$

where $I_{dc,load}$ and $I_{ac,load}$ are absorbed current by DC loads and AC loads, respectively. I_{pv} and I_{wt} are generated current by PV and WT, respectively. If $I_0 > 0$, there is a power deficit in DC microgrids and GFUs need to supply power, while a power surplus occurs in DC microgrids and GFUs need to absorb power if $I_0 < 0$.

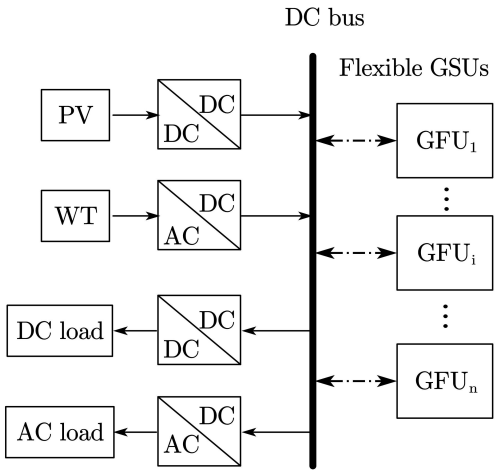

Fig. 1. Configuration of DC microgrids with different GFUs

Generally speaking, a GFU consists of a DC power source and a power electronic device, the former provides a power supply and the latter regulates the power interaction between the power source and DC bus. The detailed schematic of a GFU is illustrated in Fig.2 (a), where V_{si} is output voltage of i-th DC power source, v_i is i-th GFU converter output voltage, R_{0i} denotes the line resistance at i-th converter, and L denotes the inductor of all GFU converters. S_1 and S_2 denote two IGBT switches of all DC-DC converters. The power source of a GFU can be an ESS, it can also be an external DC microgrids, external AC microgrid or the utility grid (the latter two need AC-DC converters).

III. Control Strategies for GFUs and Plug-and-Play Discussion

A. Droop Control for GFUs in DC Microgrids

It is well-known that DC bus voltage is the most important power quality indicator for DC microgrids. To regulate the DC bus voltage, different control strategies are proposed for GFUs, and the droop control is widely used to regulate DC bus voltage and achieve power-sharing among GFUs simultaneously in a decentralized way. In the droop control, the converter output voltage linearly decreases with output current. The converter can be controlled in current mode or voltage mode [12], and in this study, it is controlled in current mode. The expression is given by Eq (2) and the detailed droop control algorithm is illustrated in Fig.2 (b)

$$I_i^{ref} = \frac{V^* - V_i}{R_i} \tag{2}$$

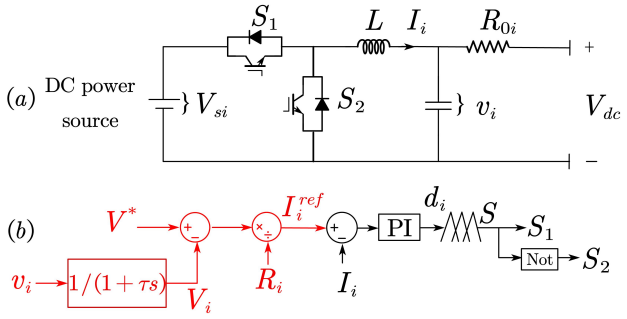

Fig. 2. Equivalent circuit of GFU and droop control algorithm for i-th GFU (a) Equivalent circuit of GFU (b) Droop control algorithm

where V^* is the nominal DC bus voltage. V_i is v_i filtered by a low-pass filter having a transfer function $1/(\tau s + 1)$, which is used to suppress the high frequency noise of v_i signal, τ is the time constant. R_i is the droop coefficient of i-th GFU. I_i^{ref} and I_i are reference and measured converter output current, respectively. d_i is the duty ratio of i-th GFU converter, V_{dc} is the measured DC bus voltage. The droop loop produces the reference of i-th converter output current I_i^{ref}, and the inner current feedback control loop tracks I_i^{ref} and generates a reference voltage for a pulse width modulation (PWM) which is used to control the bidirectional DC-DC converter. S denotes the switch signal for all converters.

The inner current loop can be viewed as '1' because it is usually designed much faster than outer loop [31], the power-sharing accuracy based on Eq (2) is given,

$$\frac{I_i}{I_j} = \frac{R_j + R_{0j}}{R_i + R_{0i}} \tag{3}$$

It is evident that the power-sharing accuracy is affected by the line resistance, and if the line resistance is much smaller than the droop coefficient, then accurate power-sharing can be achieved.

B. Advanced Control Strategies for GFUs and Discussion on Plug-and-Play

The droop control has the merits such as voltage regulation and power-sharing, and Plug-and-Play feature. However, some DC microgrid performances can not be achieved by the droop control. For example, DC microgrids supported by droop controlled GFUs will suffer from DC bus voltage deviation between V^* and V_{dc}. Further, the inertia of DC microgrids is low in power electronics dominated DC microgrids. Any disturbance introduced into the droop controlled DC microgrid will lead to a sudden change of DC bus voltage and a high RoCoV. Therefore, some advanced control strategies have been proposed to address these issues.

Secondary Control: The secondary control is proposed to eliminate the voltage deviation introduced by droop control.

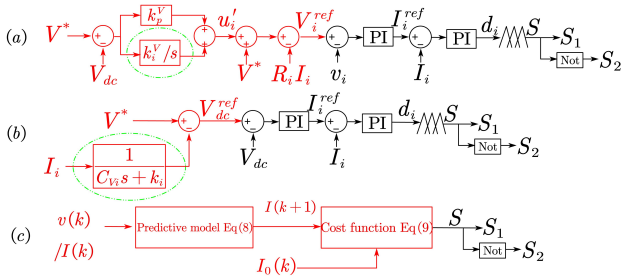

Fig. 3. Different advanced control strategies for GFUs (a) secondary control (b) virtual inertia control (c) model predictive control

As illustrated in Fig.3 (a), the DC bus voltage is used as a feedback signal and compared with V^* in secondary control [14], then secondary control term $u_i^{'}$ is generated to modify the reference of i-th GFU converter output voltage V_i^{ref}, and the dual voltage and current loop is used to track this value. The secondary control equation of i-th GFU is expressed by

$$V_i^{ref} = V^* - R_i I_i + (V^* - V_{dc})\left(k_p^V + k_i^V/s\right) \tag{4}$$

where k_p^V and k_i^V are proportional gain and integral gain of the GFU converter for voltage restoration, respectively.

Virtual Inertia Control: To increase the inertia of AC microgrids, a VSM control strategy is proposed, and the rotor equation of a VSM in AC microgrids is expressed as

$$P_{set} - P_e - D_p\left(w - w_n\right) = J\frac{dw}{dt} \tag{5}$$

where P_{set}, P_e are preset active power, electromagnetic power, respectively. w and w_n are angular frequency and nominal angular frequency, respectively. D_p and J are damping coefficient and virtual inertia in AC microgrids, respectively. To reduce RoCoV and increase the inertia of DC microgrids, a VIC was proposed in [17], where the control equation of i-th bidirectional DC-DC converter is expressed in Eq (6) by analogizing to the VSM,

$$I_{set} - I_i - k_i\left(V_{dc}^{ref} - V^*\right) = C_{Vi}\frac{dV_{dc}^{ref}}{dt} \tag{6}$$

where k_i and C_{Vi} are damping coefficient and virtual inertia provided by i-th GFU, respectively. I_{set} is the preset current and V_{dc}^{ref} is the reference of DC bus. If $I_{set} = 0$, VIC equation of i-th GFU can be simplified as

$$V_{dc}^{ref} = V^* - \frac{I_i}{k_i + C_{Vi}s} \tag{7}$$

The detailed control algorithm of VIC is illustrated in Fig.3 (b), where the dual voltage and current loop is introduced to track V_{dc}^{ref}.

Model Predictive Control: Besides the secondary control and VIC, other advanced control strategies have also been proposed for GFUs to achieve an even more improved DC microgrid performance, like MPC, FLC, ANN-based control, etc. In this study, MPC works with the power buffer as an example of these advanced control algorithms to demonstrate the effectiveness of the power buffer based control scheme for DC microgrids in retaining the Plug-and-Play functionality of GFUs with more improved DC microgrid performance.

MPC determines the sequence of the control signals at each sampling instant by optimizing a cost function. This cost function minimizes the error between the predictive output and reference output considering the physical constraints and limitations [32]. In the DC microgrids, GFUs usually allow bidirectional power flow to compensate the power mismatch between RESs and loads. Generally speaking, the DC bus voltage is often used as an indicator for power mismatch, and GFUs are usually controlled in the voltage mode and the voltage references for GFUs are often obtained from a PI controller which is fed with the DC bus voltage deviation. To compensate power mismatch and regulate DC bus voltage quickly, more advanced methods such as MPC have also been proposed, for example, authors in Reference [19] proposed a control scheme, where only one GFU is connected to the DC microgrid, and the current reference of GFU is calculated by adding the output currents of RESs and loads together. i.e., $I^{ref}(k+l|k) = I_0(k)$ as defined in Eq (1), then this reference current is tracked by the MPC controller. Hence, the next time GFU current at next time instant is predicted by

$$I(k+1) = \begin{cases} I(k) + (V_s - v(k))\,T_s/L & \text{if } S = 1 \\ I(k) - v(k)\,T_s/L & \text{if } S = 0 \end{cases} \tag{8}$$

where T_s is the sampling time. V_s is the output voltage of DC power source, v and I are GFU converter output voltage and current, respectively. In their work [19] only one GFU is connected to the DC microgrid, the subscripts 'i' in the V_{si}, v_i and I_i are omitted. The cost function is obtained by minimizing the differences between the reference current values and the predicted current values over the N_p sampling periods, i.e.,

$$J_{cost} = \sum_{l=1}^{N_p}\left(I^{ref}(k+l|k) - I(k+l|k)\right)^2 \tag{9}$$

where N_p is the prediction horizons. N_p is set to 1 in the study. The detailed control algorithm with MPC is illustrated in Fig.3 (c).

Discussions on Plug-and-Play Functionality: As illustrated in Fig.3, the time-dependent term 'integrator' (in green cycle) is introduced in the first PI controller to determine V_i^{ref} in secondary control. The VIC can be considered as a 'droop control', where the 'droop coefficient' is $1/(k + C_V s)$, which is not a constant and changes with time. Assuming two GFUs are connected in DC microgrid, they are controlled with same control strategy (secondary control/ VIC) and with identical system parameters (power source capacity, converter circuit parameters, etc). Two GFUs are supposed to play the same role in compensating power mismatch. However, the controller performance of two GFUs will be affected by the time they are connected to the DC microgrid. Assuming GFU_2 is connected to the DC microgrid later than GFU_1, as the DC bus voltage is already restored by GFU_1, the value of 'integrator' in GFU_2 equals 0 as illustrated in Fig.4 (a) unless the DC bus voltage deviation occurs. Likewise, the values of the 'droop coefficient' for two GFUs in the VIC are also different as shown in Fig.4 (b) due to different GFU connection time. Taking the connection time of GFU_2 as the initial time, the

initial value of 'droop coefficient' for GFU_2 equals 0, this will cause huge current circulation between GFU_1 and GFU_2. Different values for the 'integrator' or 'droop coefficient' lead to unequal power-sharing among GFU_1 and GFU_2, therefore, the Plug-and-Play functionality of GFUs is lost when they are controlled with secondary control or VIC. The tests in Section V will further confirm the issue raised here.

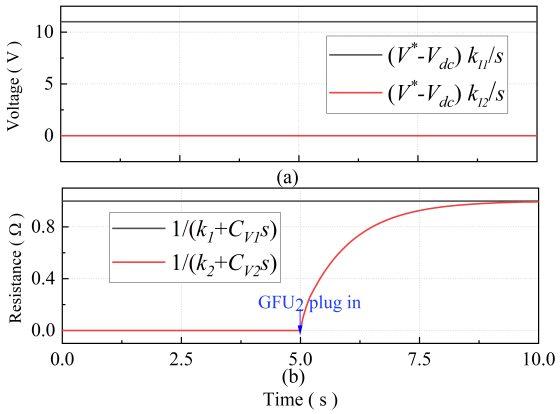

Fig. 4. The value of time-dependent terms in secondary control and VIC (a) 'integrator' in secondary control (b) 'droop coefficient' in VIC

To achieve power-sharing between the two aforementioned GFUs, one straightforward approach is to calculate the average current of all GFUs, then GFUs compare their respective currents with the average current to generate voltage correction term, like [33]. However, calculating the average current requires communication among GFUs, with the Plug-and-Play feature is inevitably lost. Another approach is to reset these time-dependent terms when a new GFU is plugged in, but this will introduce disturbances to the DC microgrids and even make the microgrid lose control.

For other advanced control strategies like MPC/FLC/ANN-based control, they usually work in a centralized way, and the information of all DERs needs to be collected in the controller design. Therefore, the control strategies of all GFUs need to be redesigned if a new DER is connected or disconnected. Hence, they also do not have the Plug-and-Play functionality. Based on the aforementioned analysis, a power buffer based control framework is proposed to restore the Plug-and-Play feature of GFUs when advanced control strategies are applied, the details are given in Section IV.

IV. Power Buffer Based Control Framework for DC Microgrids

As elaborated earlier, the droop control has the Plug-and-Play feature for all GFUs but it can not achieve the aforementioned DC microgrid performances. On the other hand, advanced control strategies are able to achieve better DC microgrid control performances, such as secondary control, VIC, and MPC. However, the Plug-and-Play feature of GFUs is lost. To address the dilemma and combine the advantages of both the droop control and advanced control strategies, a power buffer based control framework is proposed in this section.

A. The Principle of Power Buffer

The power buffer is a device that combines a bidirectional DC-DC converter and a capacitor C_{pbc}. As illustrated in Fig.5 (a), the power buffer in this study is introduced as an interface between the GFUs and DC bus. Instead of connecting GFUs in DC bus directly, GFUs are connected to the power buffer in the proposed framework, where all GFUs are controlled by the droop control, their expressions are given by

$$I_i^{ref} = \frac{V_{pbc}^* - V_i}{R_i} \tag{10}$$

where V_{pbc}^* is the nominal power buffer capacitor voltage. The voltage deviation between V_{pbc}^* and V_i drives the GFUs supply/absorb power, and power-sharing between GFUs is achieved. The detailed control algorithm for GFUs is illustrated in Fig.5 (b), and in order to reduce the voltage and current fluctuations at the system transient stage, especially during the system start-up, output current limit $\pm I_{limit}$ is introduced to limit converter output current. Further, the over voltage protection and inrush current protection in Chapter 4 of [34] are introduced in the system protection, which are widely used for converter protection to prevent any possible over voltage and over current occurring in the converter operation. If the protection is activated, the normal operation of converter will be interrupted, the threshold for triggering the over voltage and inrush current protection is often high than the rated values for the voltage and current at the transient stage. With the support of the droop controlled GFUs, C_{pbc} can be considered as a power source, it has a stable voltage and can provide a bidirectional power supply for the reliable operation of power buffers.

As elaborated in Eq (3), the accurate power-sharing can be achieved if $R_i >> R_{oi}$ is satisfied, but a too large droop coefficient will cause a huge voltage deviation. Fortunately, unlike the DC bus, since no loads or RESs are connected to C_{pbc} and the voltage quality of C_{pbc} can be sacrificed, therefore a large power buffer capacitor voltage deviation ΔV_{pbc} ($\Delta V_{pbc} = \left|V_{pbc}^* - V_{pbc}\right|$) is acceptable, where V_{pbc} is measured power buffer capacitor voltage as shown in Fig.5. Therefore, we can choose a large enough R_i to achieve accurate power-sharing. In this study, a step-down DC-DC converter is used, and the lowest V_{pbc} should be greater than V^*. Hence, the maximum ΔV_{pbc} should be smaller than $V_{pbc}^* - V^*$, yielding

$$\Delta V_{pbc}^{max} < V_{pbc}^* - V^* \tag{11a}$$

$$R_{eq} < \Delta V_{pbc}^{max} / \left(I_{pb} d_{pb}\right) \tag{11b}$$

where ΔV_{pbc}^{max} is maximum voltage deviation on power buffer capacitor, $I_{pb}d_{pb}$ is the current amount absorbed by the power buffer from C_{pbc}, $R_{eq} = 1/\sum_{i=1}^{n}(1/R_i)$, is the equivalent droop coefficient. Once R_{eq} is known, R_i can be selected according to respective GFU capacity.

Based on the specific requirement for the DC microgrid performances, e.g., zero steady-state DC bus voltage deviation, low RoCoV, and fast DC bus voltage regulation, a specific advanced control strategy can be introduced. Instead of applying

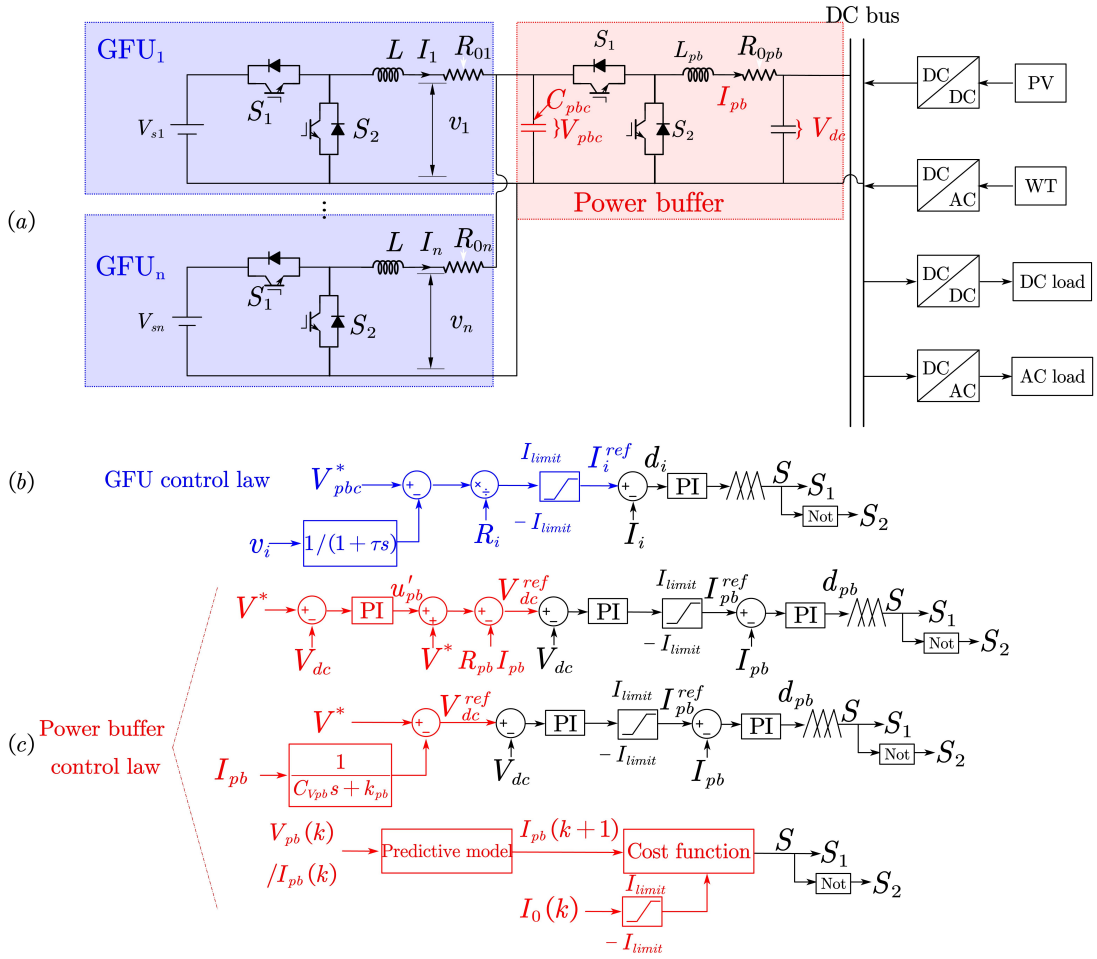

Fig. 5. Power buffer based control framework for Plug-and-Play of GFUs (a) DC microgrids configuration with power buffer (b) control algorithm of GFUs (c) control algorithm of power buffer

the specific advanced control strategy to GFUs, it is applied to the power buffer. With this scheme, the power buffer is able to control the power flow between the DC microgrid and the capacitor C_{pbc}. Note that C_{pbc} is supported by GFUs, hence, the power mismatch of the DC microgrid can be actively managed by GFUs through the power buffer. According to the power buffer based control framework, the control equations/ MPC cost function of power buffer are modified are given in Eq (12) and the control algorithm for the power buffer is illustrated in Fig.5 (c).

$$V_{dc}^{ref} = V^* - R_{pb}I_{pb} + (V^* - V_{dc})\left(k_{ppb}^V + k_{ipb}^V/s\right) \quad (12a)$$

$$V_{dc}^{ref} = V^* - \frac{1}{k_{pb} + C_{Vpb}s} I_{pb} \quad (12b)$$

$$J_{cost} = \sum_{l=1}^{N_p} \left(I_{pb}^{ref}\left(k+l|\,k\right) - I_{pb}\left(k+l|\,k\right)\right)^2 \quad (12c)$$

where I_{pb} and I_{pb}^{ref} are the power buffer output current and its reference, respectively. R_{pb} and R_{0pb}, respectively, are droop coefficient and line resistance between power buffer converter and DC bus. k_{ppb}^V and k_{ipb}^V are proportional gain and integral gain for voltage restoration of the power buffer, respectively. $u_{pb}^{'}$ is secondary term for power buffer. k_{pb} and C_{Vpb} are damping coefficient and virtual inertia provided by power buffer, respectively. d_{pb} is the duty ratio of power buffer converter. Output current limit $\pm I_{limit}$ is also introduced for the power buffer converter.

In summary, by applying the droop control to GFUs while applying the advanced control strategies to the power buffer, better DC microgrid performances and the Plug-and-Play feature of GFUs can all be achieved simultaneously, which otherwise can not be achieved by advanced control strategies alone. It is worth noting that within this proposed control framework, power buffer can not only work with the aforementioned advanced control strategies in this paper, but also with other advanced control strategies. In other words, within this power buffer based control framework, the control strategies adopted for the power buffer can be selected based on the specifically required DC microgrid performances.

In the practical implementation of power buffer, the following procedure should be followed to keep the safe operation of the whole system. First, connect GFUs to the power buffer capacitor and regulate the capacitor voltage to the preset value. Second, connect the power buffer to the DC bus and regulate DC bus voltage to the preset value. Finally, Plug in/out GFUs.

It should be noted that the power demand from the equivalent load is compensated by GFUs through the power buffer. Hence, the power rating of power buffer converter should be at least 120% of the maximum power demand from the equivalent load to ensure the safe operation of the converter in the power buffer.

B. Small-Signal Stability Analysis

B.1 Power Buffer Controlled by Conventional PI Controller

The small-signal stability is conducted to investigate the system stability and the impact of device and controller parameters on the system dynamics. The impact of different parameters on the system dynamics can be assessed by analyzing eigenvalues locus and their corresponding dominant state variables. In the B.1, the secondary control is introduced in the small-signal stability analysis as an example. Based on the electric circuit in the Fig.5 (a), the following equations can be obtained.

$$C_{dc}\dot{V}_{dc} = I_{pb} - I_0 \tag{13a}$$

$$L_{pb}\dot{I}_{pb} = V_{pbc}d_{pb} - R_{0pb}I_{pb} - V_{dc} \tag{13b}$$

where C_{dc} is the DC bus capacitance. To reduce the complexity of small-signal analysis, the secondary control is modified by Eq (14), where the measured DC bus voltage is used as feedback and compared with its nominal value to generate the reference of power buffer output current in the outer voltage loop, then it is tracked by an inner current loop

$$I_{pb}^{ref} = (V^* - V_{dc})\left(k_{ppb}^V + k_{ipb}^V/s\right) \tag{14a}$$

$$d_{pb} = \left(I_{pb}^{ref} - I_{pb}\right)\left(k_p^I + k_i^I/s\right) \tag{14b}$$

For simplicity, k_p^I and k_i^I denote the proportional gain and integral gain in current loop of all converters, respectively. With the electric circuit of GFUs, we have

$$L\dot{I}_i = V_{si}d_i - V_{pbc} - I_iR_{0i} \tag{15a}$$

$$C_{pbc}\dot{V}_{pbc} = \sum_{i=1}^{n} I_i - I_{pb}d_{pb} \tag{15b}$$

$$v_i = V_{pbc} + I_iR_{0i} \tag{15c}$$

Based on GFU control strategy, it yields

$$I_i^{ref} = \left(V_{pbc}^* - V_i\right)/R_i \tag{16a}$$

$$V_i = 1/\left(1+\tau s\right)v_i \tag{16b}$$

$$d_i = \left(I_i^{ref} - I_i\right)\left(k_p^I + k_i^I/s\right) \tag{16c}$$

Linearizing Eq (13) to Eq (16) at the equilibrium point, it yields

$$x = A\dot{x} \tag{17}$$

where $x = \left[\Delta V_{dc}, \Delta I_{pb}, \Delta I_{pb}^{ref}, \Delta d_{pb}, \Delta V_{pbc}, \Delta \boldsymbol{V}, \Delta \boldsymbol{I}, \Delta \boldsymbol{d}\right]^T$. $\Delta \boldsymbol{V} = [\Delta V_1, \Delta V_2, \cdots, \Delta V_n]^T$, $\boldsymbol{I} = [\Delta I_1, \Delta I_2, \cdots, \Delta I_n]^T$, $\boldsymbol{d} = [\Delta d_1, \Delta d_2, \cdots, \Delta d_n]^T$. Δx represents small perturbations of state variable x. A is expressed by Eq (18), $\mathbf{1_n}$ and $\mathbf{0_n}$ is n-th order vector with all elements equal to 1 and 0, respectively. $\mathbf{0_{n\times n}}$ is $n \times n$ matrix with all elements equal to 0. $\boldsymbol{I_n}$ is the n-th order identity matrix. $\bar{V}_{pbc}$ and $\bar{I}_{pb}$ are the values of V_{pbc} and I_{pb} at equilibrium point, respectively. D_{pb} is the value of d_{pb} at equilibrium point.

$$l_{41} = -k_p^I k_{ipb}^V + k_p^I/L_{pb}$$
$$l_{42} = -\left(k_p^I k_{ppb}^V/C_{dc} + k_i^I\right)$$
$$\boldsymbol{l_{67}} = -\mathrm{diag}\left(R_{01}, \cdots, R_{0n}\right)/\tau$$
$$\boldsymbol{l_{77}} = -\mathrm{diag}\left(R_{01}, \cdots, R_{0n}\right)/L$$
$$\boldsymbol{l_{78}} = \mathrm{diag}\left(V_{s1}, \cdots, V_{sn}\right)/L$$
$$\boldsymbol{l_{85}} = \left[k_p^I/L - k_p^I/\left(\tau R_1\right), \cdots, k_p^I/L - k_p^I/\left(\tau R_n\right)\right]^T$$
$$\boldsymbol{l_{86}} = \mathrm{diag}\left[\left(k_p^I/\tau - k_i^I\right)/R_1, \cdots, \left(k_p^I/\tau - k_i^I\right)/R_n\right]$$
$$\boldsymbol{l_{87}} = \mathrm{diag}\begin{bmatrix} k_p^I R_{01}/\left(\tau R_1\right) - k_i^I + k_p^I R_{01}/L, \\ \cdots, k_p^I R_{0n}/\left(\tau R_n\right) - k_i^I + k_p^I R_{0n}/L \end{bmatrix}$$
$$\boldsymbol{l_{88}} = \mathrm{diag}\left(-k_p^I V_{s1}/L, \cdots, -k_p^I V_{sn}/L\right)$$

TABLE I
EIGENVALUE AND DOMINANT STATE VARIABLES

λ	Dominant state variable
λ_1	Δd_{pb}
λ_2/λ_3	Δd_1 and Δd_2
λ_4/λ_5	ΔI_{pb}
λ_6	ΔV_{dc}
λ_7/λ_8	ΔI_1 and ΔI_2
λ_9	ΔV_1 and ΔV_2
λ_{10} /λ_{11}	ΔI_1 and ΔI_2

It can be observed from Eq (17) that system is a 3n+5 order system. In this study, 2 GFUs are used in the system, i.e., $n = 2$, the location of eigenvalues is illustrated by Fig.6 and the corresponding dominant state variables of different eigenvalues are shown in Table I. Fig.6 shows that all eigenvalues are located in the left-panel, which means the system is stable. In Table I, λ_1, λ_4, λ_5, λ_6 are dominated by the state variables of the power buffer converters, while the left are dominated by the state variables of GFUs.

Fig. 7 illustrates the impact of different device and controller parameters on the system dynamics, where the blue stars represent where the eigenvalues move from and red stars represent where the eigenvalues stop, and the arrows represent the movement of eigenvalues as these parameters vary. In Fig.7 (a), λ_4 and λ_5 moves to imaginary axis with C_{dc} increases, which shows that the increase of C_{dc} slows down the response speed of the corresponding state variable ΔI_{pb}. While the eigenvalues dominated by the state variables of GFUs (like λ_7, λ_8, λ_9, λ_{10}, λ_{11}) keep unchanged and stay at same location with Fig.6, thus, the change of C_{dc} does not impact the dynamics of of GFU state variables. Similarly, Fig. 7 (b) illustrates the movement of λ_7 and λ_8 moves as C_{pbc} increases, while the state variables of power buffer (like λ_4, λ_5, λ_6) keep unchanged and stay at the same location as shown in Fig. 6. In Fig.7 (c), the increase of L_{pb} slows down the response speed of Δd_{pb}. The increase of L reduces the response speed of $\Delta d_1/\Delta d_2$, the results are not presented here because they are similar with L_{pb} changes. Also, the L_{pb} (L) does not change the dynamics of state variables of GFUs (power buffer). Fig.7 (d) shows that λ_6 moves away imaginary axis as k_{ipb}^V increases

$$A=\begin{pmatrix} 0 & 1/C_{dc} & 0 & 0 & 0 & \mathbf{0_n^T} & \mathbf{0_n^T} & \mathbf{0_n^T} \\ -1/L_{pb} & -R_{pb}/L_{pb} & 0 & \bar{V}_{pbc}/L_{pb} & D_{pb}/L_{pb} & \mathbf{0_n^T} & \mathbf{0_n^T} & \mathbf{0_n^T} \\ -k_{ipb}^V & -k_{ppb}^V/C_{dc} & 0 & 0 & 0 & \mathbf{0_n^T} & \mathbf{0_n^T} & \mathbf{0_n^T} \\ l_{41} & l_{42} & k_i^I & -k_p^I\bar{V}_{pbc}/L_{pb} & -k_p^I D_{pb}/L_{pb} & \mathbf{0_n^T} & \mathbf{0_n^T} & \mathbf{0_n^T} \\ 0 & -D_{pb}/C_{pbc} & 0 & 0 & 0 & \mathbf{0_n^T} & \mathbf{1_n^T}/C_{pbc} & \mathbf{0_n^T} \\ \mathbf{0_n} & \mathbf{0_n} & \mathbf{0_n} & \mathbf{0_n} & \mathbf{1_n}/\tau & -\boldsymbol{I_n}/\tau & \boldsymbol{l_{67}} & \mathbf{0_{n\times n}} \\ \mathbf{0_n} & \mathbf{0_n} & \mathbf{0_n} & \mathbf{0_n} & -\mathbf{1_n}/L & \mathbf{0_{n\times n}} & \boldsymbol{l_{77}} & \boldsymbol{l_{78}} \\ \mathbf{0_n} & \mathbf{0_n} & \mathbf{0_n} & \mathbf{0_n} & \boldsymbol{l_{85}} & \boldsymbol{l_{86}} & \boldsymbol{l_{87}} & \boldsymbol{l_{88}} \end{pmatrix} \tag{18}$$

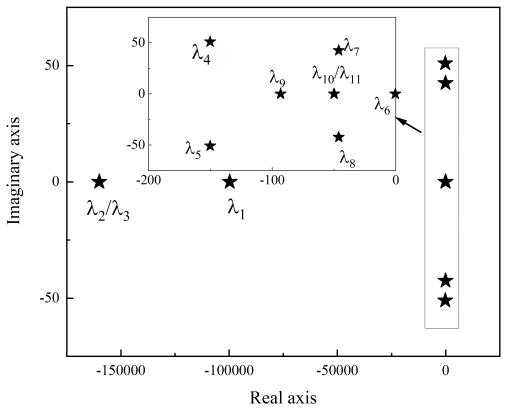

Fig. 6. Location of eigenvalues

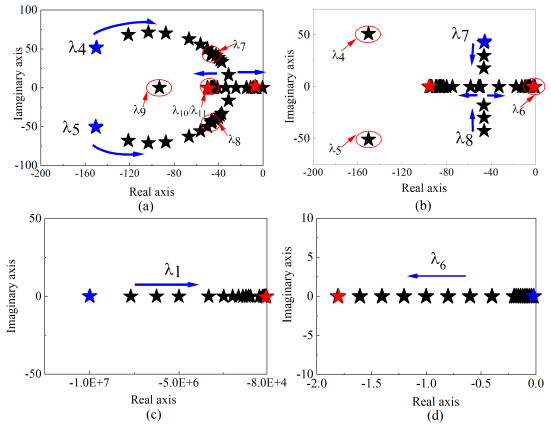

Fig. 7. Eigenvalue locus (a) with C_{dc} increase (b) with C_{pbc} increase (c) with L_{pb} increase (d) with k_{ipb}^V increase

while other eigenvalues keep unchanged, thus, the DC bus regulation speed can be increased by increasing the controller parameters.

In summary, although the GFU and power buffer are series connected through C_{pbc}, the change of parameters in power buffer has no impact on the state variables of the GFUs and vice versa. Therefore, the converters design can follow the conventional converter design guideline. The L_{pb}/L is designed according to the current ripple requirements, while the C_{pbc}/C_{dc} should be designed according to the voltage ripple requirements. In the following, the design of L_{pb} and C_{dc} are used as an example, their ranges are given in the following equations [35]

$$L_{pb} > V_{dc}\left(1-d_{pb}\right)/\left(fI_{rip}\right) \tag{19a}$$

$$C_{dc} > V_{dc}\left(1-d_{pb}\right)/\left(8L_{pb}f^2V_{rip}\right) \tag{19b}$$

where f is the switching frequency of converters, V_{rip} and I_{rip} are allowed voltage ripple on DC bus and current ripple on the inductor, respectively. Based on the stability analysis, larger controller proportional/integral gains lead to a faster converter dynamics, and it is well-acknowledged that current loop bandwidth is usually designed at 1/10 of the switching frequency, and the outer loop bandwidth is selected at less than 1/10 of the current loop in the controller design [36]. Therefore, given the known device impedance, the controller gains should be selected to satisfy the bandwidth requirements.

B.2 Power Buffer Controlled by MPC Controller

In the B.2, the stability analysis is conducted where the power buffer is controlled by the MPC controller. In some MPC applications, a short prediction horizon may cause system unstable. Hence, a long prediction horizon is necessary to achieve a better control performance and avoid the stability issues, even though it will introduce more computation burden in solving the optimization problem. To better elaborate the stability issue caused by a short prediction horizon, the boost converter controlled in the voltage mode is used as an example. Assuming a boost converter is used to build the power buffer, and MPC is used for direct V_{dc} tracking, then it is easy to derive the transfer function between V_{dc} and d_{pb} as given below

$$\frac{\Delta V_{dc}}{\Delta d_{pb}}=\frac{\bar{V}_{pbc}}{{D_{pb}}'^2}\,\frac{R_{laod}{D_{pb}}'^2-sL_{pb}}{s^2L_{pb}C_{dc}R_{laod}+sL_{pb}+R_{laod}{D_{pb}}'^2} \tag{20}$$

where R_{load} is the resistance of the equivalent load connected to the DC bus, ${D_{pb}}' = 1-D_{pb}$. Eq (20) shows that the transfer function has a right half-panel zero, which implies that the V_{dc} has a non-minimum phase behavior with d_{pb} [37], as illustrated in Fig.8 (a), the output voltage first decreases and then increases with the step change (step increase) of d_{pb} at the step k. It is well-known that d_{pb} is supposed to increase to track the increase of reference of V_{dc}. However, MPC controller is not able to 'see' that the increase of d_{pb} leads to a increase of V_{dc} when the prediction horizon is less than l_2, then the controller will make wrong action and make the whole system unstable.

In this paper, a buck converter is actually used to construct the power buffer in the proposed control framework and it works at the current tracking mode, the transfer function between I_{pb} and d_{pb} is expressed by

$$\frac{\Delta I_{pb}}{\Delta d_{pb}} = \frac{\bar{V}_{pbc}\left(1+sC_{dc}R_{laod}\right)}{s^2L_{pb}C_{dc}R_{laod}+sL_{pb}+R_{laod}} \tag{21}$$

Unlike the boost converter controlled in the voltage mode, there is no right half-panel zero in Eq (21), and it can be considered as a minimum phase system. The response of I_{pb} with step change of d_{pb} at the step k is illustrated in the Fig.8 (b), one step ahead is sufficient for MPC controller 'see' the increase of I_{pb} as d_{pb} increase. Hence, I_{pb} can track its reference (I_0) quickly with MPC and while the instability issue is avoided.

To investigate the stability of the whole system, $I_{pb} = I_0$ is assumed considering fast reference current tracking with advanced MPC. With the electric circuit of GFUs, it yields

$$L\dot{I}_i = V_{si}d_i - V_{pbc} - I_iR_{0i} \tag{22a}$$

$$C_{pbc}\dot{V}_{pbc} = \sum_{i=1}^{n} I_i - I_0d_{pb} \tag{22b}$$

$$v_i = V_{pbc} + I_iR_{0i} \tag{22c}$$

Combing the control law for GFUs in Eq (16) and linearizing them at the equilibrium point, it yields

$$x^{'} = A^{'}\dot{x}^{'} \tag{23}$$

where $x^{'} = [\Delta V_{pbc}, \Delta \boldsymbol{V}, \Delta \boldsymbol{I}, \Delta \boldsymbol{d}]^T$, and $A^{'}$ is expressed by

$$A^{'} = \begin{pmatrix} 0 & \mathbf{0_n^T} & \mathbf{1_n^T}/C_{pbc} & \mathbf{0_n^T} \\ \mathbf{1_n}/\tau & -\boldsymbol{I_n}/\tau & \boldsymbol{l_{23}^{'}} & \mathbf{0_{n\times n}} \\ -\mathbf{1_n}/L & \mathbf{0_{n\times n}} & \boldsymbol{l_{33}^{'}} & \boldsymbol{l_{34}^{'}} \\ \boldsymbol{l_{41}^{'}} & \boldsymbol{l_{42}^{'}} & \boldsymbol{l_{43}^{'}} & \boldsymbol{l_{44}^{'}} \end{pmatrix} \tag{24}$$

$\boldsymbol{l_{23}^{'}} = \boldsymbol{l_{67}}$, $\boldsymbol{l_{33}^{'}} = \boldsymbol{l_{77}}$, $\boldsymbol{l_{34}^{'}} = \boldsymbol{l_{78}}$, $\boldsymbol{l_{41}^{'}} = \boldsymbol{l_{85}}$, $\boldsymbol{l_{42}^{'}} = \boldsymbol{l_{86}}$, $\boldsymbol{l_{43}^{'}} = \boldsymbol{l_{87}}$, $\boldsymbol{l_{44}^{'}} = \boldsymbol{l_{88}}$.

Fig.9 illustrates the eigenvalue locus as C_{pbc} increases based on the Eq (23), and it is shown that all eigenvalues are located in the left half-panel and hence the system is stable. It is also shown that the eigenvalues move toward imaginary axis, which means that the increase of C_{pbc} slows down the system response.

V. Hardware-in-loop Test Results and Discussions

To validate the proposed power buffer based control framework, the HIL real-time tests are conducted using the Typhoon HIL-604 platform. This ultra-high fidelity HIL device consists of 8-core processors able for real-time emulation of up to 8 converters, and can test the controller with 20 ns PWM resolution. It can also emulate power stage with up to 2 MHz update rate. This device can interface to external hardware controllers via its 64 analog outputs, 32 analog inputs, 64 digital inputs, and 64 digital outputs. As illustrated in Fig.10, the whole system (converters, DC power source) is emulated by typhoon HIL-604, while the controller for the real-time

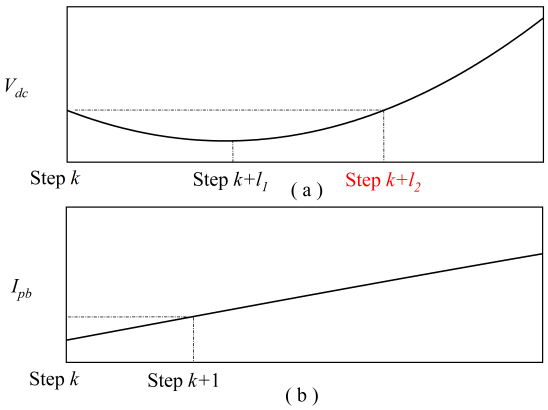

Fig. 8. System response with step change of d_{pb} (a) V_{dc} response (b) I_{pb} response

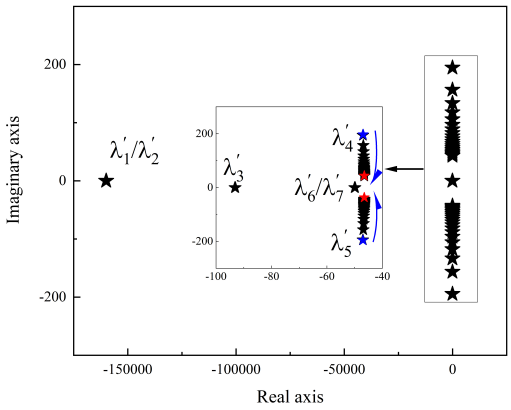

Fig. 9. Eigenvalue locus as C_{pbc} increases when power buffer is controlled by MPC

emulated system is implemented using a Texas Instruments TI LaunchPad (LAUNCHXL-F28069M), which is interfaced with the typhoon HIL device through a Launchpad interface. The controller communicates the emulated system through 16-ADC channels, then sends PWM signals back to typhoon HIL device.

TABLE II
System and control parameters used in HIL tests

Parameters	Value	Parameters	Value
V^*	380 V	V_{pbc}^*	500 V
$V_{si}, (i=1,2)$	750 V	$R_i, (i=1,2)$	5 Ω
R_{01}	0.5 Ω	R_{02}	0.2 Ω
L	0.01 H	L_{pb}	0.01 H
C_{dc}	0.01 F	C_{pbc}	0.01 F
τ	0.01 s	ΔV_{pbc}^{max}	100 V
C_{Vpb}	1	k_{pb}	1
$C_{Vi}, (i=1,2)$	1	$k_i, (i=1,2)$	1
k_{ppb}^V	5	k_{ipb}^V	5
k_p^I	2	k_i^I	100
N_p	1	T_s	1e-5 s

Three cases are used to validate the proposed control

framework, where the secondary control, VIC and MPC are introduced to work with power buffer control strategy. The parameters for the system and controller used in the study are listed in Table II. And both the execution time step in the TI LaunchPad and running time step are set as 1e-5 s, and the data is saved and presented at SCADA panel, the step of which is 1e-4 s.

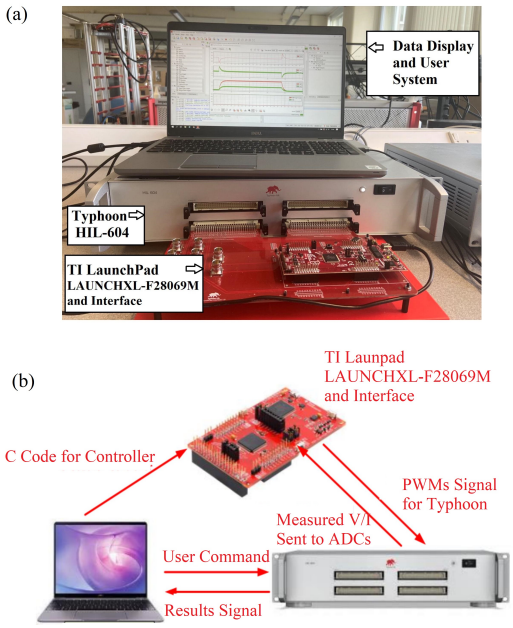

Fig. 10. HIL tests (a) Experimental set-up (b) Device operation details

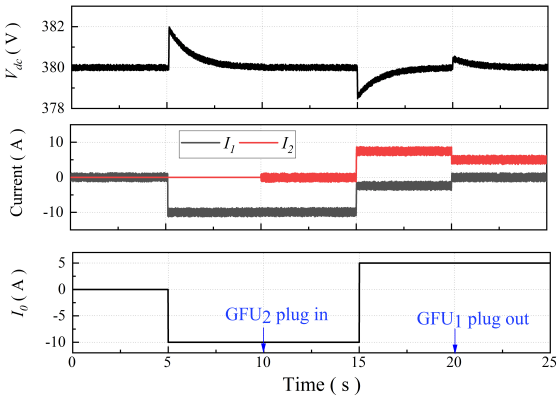

Fig. 11. GFUs regulated by secondary control without power buffer

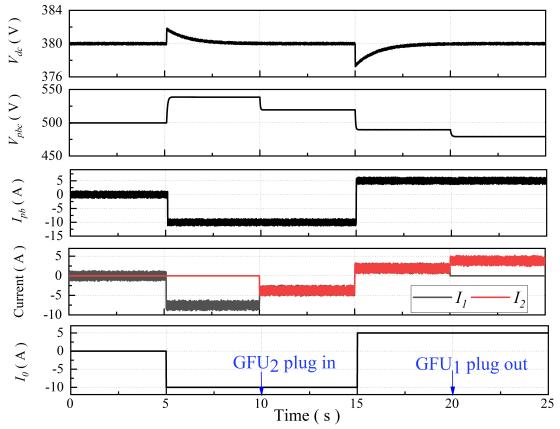

Fig. 12. DC microgrid regulated by secondary control with power buffer

A. Secondary Control

A.1 Comparison between with/without power buffer

In this sub-case, DC bus voltage is regulated with secondary control, and the comparison results with and without power buffer are presented. Fig.11 illustrates the DC bus voltage regulation and power-sharing of GFUs without power buffer. From 0 s to 10 s, only GFU_1 is connected in DC microgrids, GFU_2 is plugged in at 10 s and GFU_1 is plugged out at 20 s. Perturbation is introduced to I_0 at 5 s and 15 s. It can be observed that DC bus voltage is regulated to V^* (380 V) at steady-state but the power-sharing between two GFUs is not achieved. The reason has been explained in Section III, the values of 'integrator' are different due to different GFUs connection time, which disabled the Plug-and-Play functionality of two GFUs.

While as shown in Fig.12, when the power buffer is introduced, the power-sharing among two GFUs is achieved immediately when GFU_2 is connected at 10 s. Note large R_i is adopted to achieve power-sharing among GFUs and large V_{pbc} voltage deviation is introduced, but it is acceptable because no loads or RESs are connected to C_{pbc}. The other advantage of the power buffer strategy is that there is no DC bus voltage fluctuation when GFUs plug in/out, and voltage fluctuates only at the time that I_0 is perturbed. On the contrary, when the power buffer is not introduced, Fig.11 shows the voltage fluctuation occurs when GFU_1 is plugged out.

A.2 Comparison with existing control strategy

In this sub-case, the control strategy in [16] is tested and compared with the proposed control framework. To achieve zero voltage error regulation and accurate current-sharing, Reference [16] introduces communication links between GFUs, which inevitably reduces the their flexibility. Further, the disconnection of some GFUs will disable the communication network, then the control objectives can not be achieved consequently. Four GFUs are used in this case study, which are controlled by droop control in the proposed control framework. The communication network of the control strategy in [16] is shown by Fig.13. It also shows the performances with two different control strategies. From 0 s to 5 s, four GFUs are connected into DC microgrids, and DC bus voltage gradually approaches the nominal value and current-sharing are achieved with both two different control strategies. However, the disconnection of GFU_2 and GFU_4 at 5 s leads the communication lost between GFU_1 and GFU_3 in [16], hence, their current-sharing can not be achieved. While in the proposed control framework, GFU_1 and GFU_3 achieves accurate current-sharing immediately after other two GFUs are disconnected, more importantly, unlike the control strategy in [16], the Plug out of GFU_2 and GFU_4 does not introduce any voltage fluctuation on DC bus voltage.

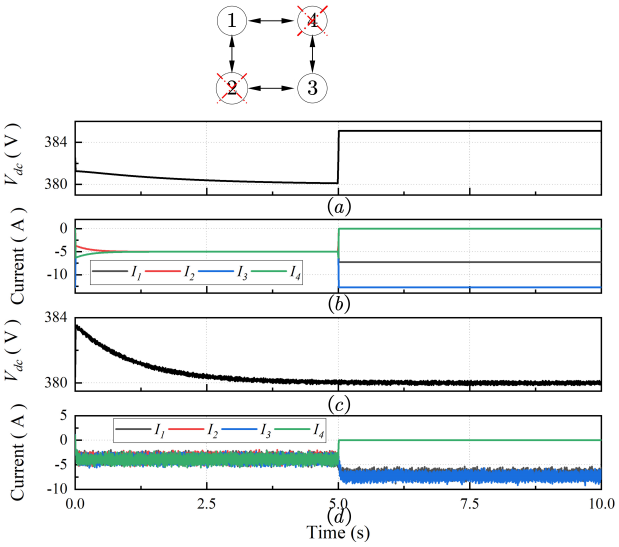

Fig. 13. Comparison between the proposed control strategy and control framework in [16] (a) DC bus voltage with [16] (b) output currents with [16] (c) DC bus voltage with the proposed control framework (d) output currents with the proposed control framework

B. Virtual Inertia Control

In this case, DC bus voltage is regulated with VIC, and the comparison results with and without power buffer are presented. Fig.14 illustrates GFUs regulated by VIC without power buffer. From 0 s to 8 s, only GFU_1 is connected in DC microgrids, GFU_2 is plugged in at 8 s and GFU_1 is plugged out at 10 s. I_0 is perturbed at 2.5 s. With VIC, the sudden change of DC bus voltage is avoided and RoCoV is reduced when I_0 is perturbed. However, the huge current surge (more than 60 A) occurs both in GFU_1 and GFU_2 when GFU_2 is plugged in, meanwhile, a sudden voltage drop is also observed at that time. The reasons are also given in Section III, VIC can be considered as a 'droop control', the 'droop coefficient' $1/(C_V s + k)$ is a time function, the initial values of 'droop coefficient' are different in two GFUs, which introduces huge current circulation.

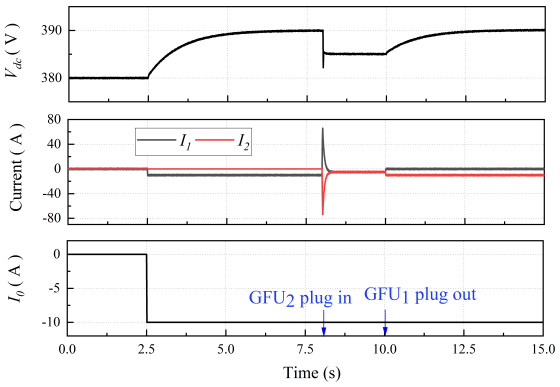

Fig. 14. GFUs regulated by VIC without power buffer

Fig.15 illustrates DC bus voltage regulation and power-sharing between GFUs with power buffer. The sudden change of DC bus voltage is avoided and RoCoV is reduced at I_0 perturbs. The power-sharing among two GFUs is achieved immediately when GFU_2 is connected at 8 s. The plug in/out of GFUs does not introduce DC bus voltage fluctuation.

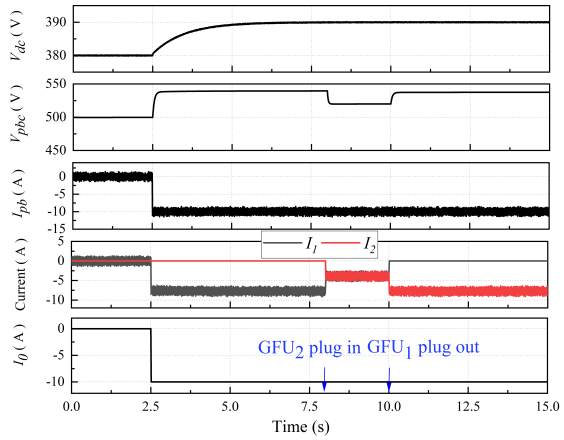

Fig. 15. DC microgrid regulated by VIC with power buffer

C. Model Predictive Control

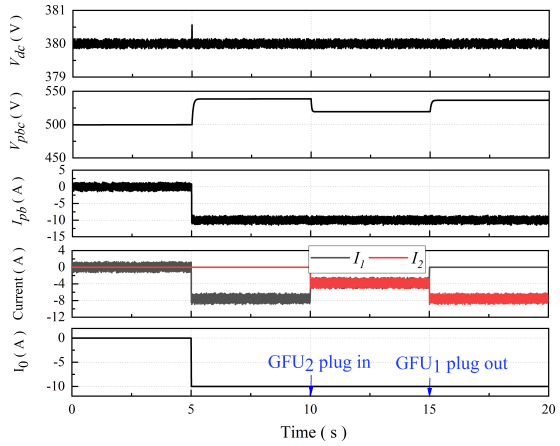

Fig. 16. DC microgrid regulated by MPC with power buffer

MPC is introduced to regulate DC microgrids in this case. The detailed MPC algorithm with power buffer is shown in Fig.6, where communication network between power buffer and RES/loads is needed to transfer their output currents. Fig.16 illustrates DC microgrid regulated by MPC with power buffer. From 0 s to 10 s, only GFU_1 is connected in DC microgrids, GFU_2 is plugged in at 10 s and GFU_1 is plugged out at 15 s. I_0 is perturbed at 5 s. With MPC, a fast DC bus regulation is achieved compared with secondary control, as MPC uses more information (currents of all RES/loads) while only DC bus voltage information is used in secondary control. It can be observed that the power-sharing among two GFUs is achieved immediately when GFU_2 is connected at 10 s. The GFU_2 support DC bus voltage by itself when GFU_1 is disconnected. There is no voltage fluctuation when GFUs plug

in/out with power buffer based control framework. If power buffer is not introduced, GFU_1 will need to know output currents of all RESs and loads and compensate their mismatch before GFU_2 is connected. The whole control strategy and communication network need to be redesigned when GFU_2 is connected. Therefore, no power buffer test is not conducted in this case.

In summary, with the power buffer based control framework, the power-sharing among all GFUs is achieved immediately when the other GFU is plugged in/out of the DC microgrids, and the specific DC microgrid performances are achieved in all three cases. The plug in/out of GFUs does not introduce DC bus voltage fluctuation. However, the power-sharing among GFUs can not be achieved and DC bus voltage regulation is affected when the other GFU is connected/disconnected without power buffer. Hence, the power buffer based framework restores Plug-and-Play functionality of GFUs when they are controlled with advanced control strategies.

VI. Experiments

To further validate the proposed control framework, an experiment with real electric circuit is conducted. The Fig.17 (a) illustrates the device set-up and Fig.17 (b) shows the detailed connection of different devices. Two 24V/20Ah batteries work as two DC sources, and the switch box and passive filter box from the Imperix are used to construct the converters. The Typhoon HIL-604 collects the voltage and current information of converters and sends PWM signal back to drive them. The step up converter is used to build 48V DC microgrid, and the secondary control is selected in the this section.

Fig.18 shows the experiment results with the proposed control framework under load change, DC bus voltage is regulated to its nominal value (48V), and the current-sharing between two GFUs are achieved. Since GFUs are droop controlled, there is a voltage deviation between V_{pbc} and its nominal value (35V). An other load is connected to the DC microgrid at 5s, it can be observed that the voltage regulation and current-sharing can still be achieved after load perturbation.

The experiment results with GFU_2 plug out are illustrated in the Fig.19, the zero-error voltage regulation and accurate current-sharing are achieved. GFU_2 is plugged out at 5s, there is no DC bus voltage fluctuation introduced and the DC microgrid is successfully supported by GFU_1 only after GFU_2 is plugged out.

VII. Conclusions

This paper has proposed a power buffer based control framework for DC microgrids to restore the Plug-and-Play feature of GFUs and achieve desired DC microgrid performances simultaneously, which otherwise can not be achieved using existing control strategies. The power buffer is a device combing a capacitor and a bidirectional DC-DC converter, it is used as an interface between the GFUs and DC bus. The principle of the proposed framework is that GFUs are regulated by the droop control while the advanced control strategies are applied to the power buffer. In this way, the Plug-and-Play of GFUs and the specific DC microgrid performance are achieved

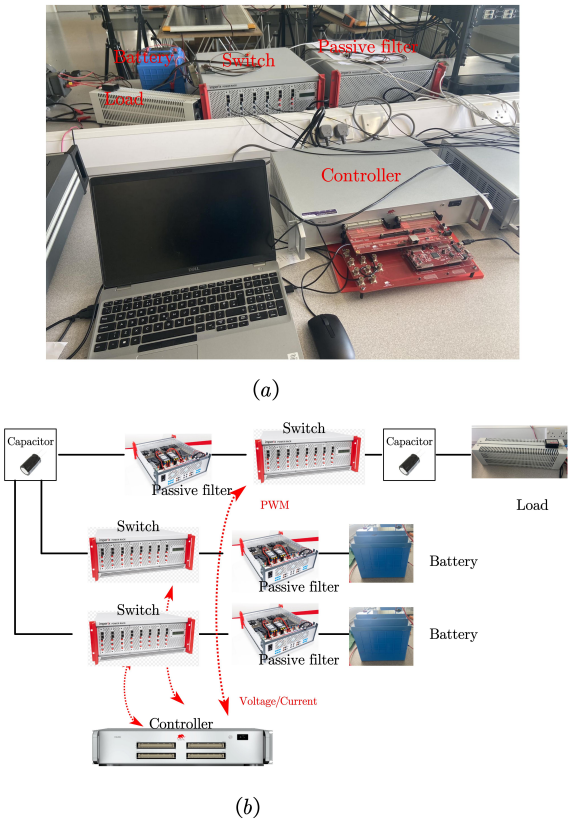

Fig. 17. Experiments (a) Experiment set-up (b) Device connection detail

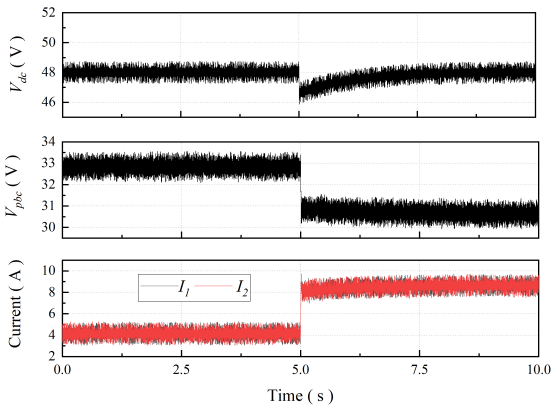

Fig. 18. Secondary control with the proposed control framework under load change

simultaneously. With the proposed control framework, GFUs are able to be plugged in/out DC microgrids seamlessly without introducing DC bus voltage fluctuation. The experimental studies with/without power buffer are conducted in HIL environment, where three different control strategies are tested in combination with the power buffer.

The test results show that the power-sharing among all GFUs are achieved immediately when GFUs are plugged in/out of the DC microgrids, and the specific DC microgrid performance is achieved with the power buffer based strategy.

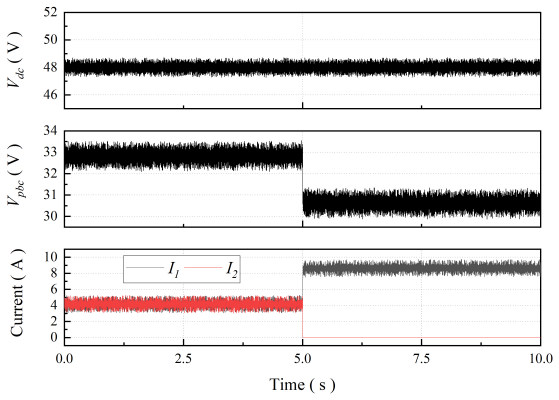

Fig. 19. Secondary control with the proposed control framework and GFU_2 plug out

Further, the plug in/out of GFUs does introduce DC bus voltage fluctuation.

It is worth noting that introduction of the power buffer device into the proposed DC microgrid control framework will inevitably increase the overall system cost. For example, in battery energy storage systems, the cost of all converters accounts for 10-20% of the total cost. In the proposed control framework, if n GFU converters are connected to a single power buffer, it is reasonable to assume that the cost of power buffer is proportional to (but smaller than) the total cost of n converters considering that the capacity of the power buffer has to match the total current and power flowing through it from all the GFU converters. Therefore, the power buffer will be an extra top-up but adding at a less significant percentage ($<$ 10-20%) of the total costs. However, the benefits are multifaceted. First, it allows dynamic forming of the DC microgrid, enabling plug-and-play of GFUs without introducing disturbances even faults to the DC microgrid operation. Second, the framework enables integration of a range of advanced control strategies to achieve desired control performances, significantly enhancing the flexibility of the controller design in DC microgrids. Finally, this framework unifies and simplifies the controller design for GFUs as all advanced controls are shifted from GFUs to the power buffer, and only a simply droop control is required for GFUs. This also allows the standardization of controller design for a variety of GFUs.

ACKNOWLEDGMENTS

Jialei SU would like to thank the China Scholarship Council for the financial support of his PhD study at University of Leeds.

This work is partially supported by the Ofgem/UKRI SIF project 'Resilient and Flexible Railway Multi-Energy Hub Networks for Integrated Green Mobility', SP Energy Network Funded project 'A holistic approach for power system monitoring to support DSO transition'.

REFERENCES

[1] D. E. Olivares, A. Mehrizi-Sani, A. H. Etemadi, and e. a. Cañizares, "Trends in microgrid control," *IEEE Transactions on Smart Grid*, vol. 5, no. 4, pp. 1905–1919, 2014.

[2] C. M. R. Lasseter, A. Akhil, "The certs microgrid concept—white paper on integration of distributed energy resources," *U.S. Dept. Energy, Lawrence Berkeley Nat. Lab., Berkeley, CA, USA, Tech. Rep.LBNL-50829*, 2002.

[3] Y. Khayat, J. M. Guerrero, H. Bevrani, Q. Shafiee, R. Heydari, M. Naderi, T. Dragicevic, J. W. Simpson-Porco, F. Dorfler, M. Fathi, and F. Blaabjerg, "On the secondary control architectures of ac microgrids: An overview," *IEEE Transactions on Power Electronics*, vol. 35, no. 6, pp. 6482–6500, 2020.

[4] R. Panigrahi, S. K. Mishra, S. C. Srivastava, A. K. Srivastava, and N. N. Schulz, "Grid integration of small-scale photovoltaic systems in secondary distribution network - a review," *IEEE Transactions on Industry Applications*, vol. 56, no. 3, pp. 3178–3195, 2020.

[5] E. Unamuno and J. A. Barrena, "Hybrid ac/dc microgrids - part ii: Review and classification of control strategies," *Renewable and Sustainable Energy Reviews*, vol. 52, pp. 1123–1134, 2015.

[6] J. Rocabert, A. Luna, F. Blaabjerg, and P. Rodríguez, "Control of power converters in ac microgrids," *IEEE Transactions on Power Electronics*, vol. 27, no. 11, pp. 4734–4749, 2012.

[7] Q. Xu, X. Hu, P. Wang, J. Xiao, P. Tu, C. Wen, and M. Y. Lee, "A decentralized dynamic power sharing strategy for hybrid energy storage system in autonomous dc microgrid," *IEEE Transactions on Industrial Electronics*, vol. 64, no. 7, pp. 5930–5941, 2017.

[8] A. S. Soliman, M. M. Amin, F. F. El-Sousy, and O. Mohammad, "Experimental validation for artificial data-driven tracking control for enhanced three-phase grid-connected boost rectifier in dc microgrids," *IEEE Transactions on Industry Applications*, pp. 1–17, 2022.

[9] M. Faisal, M. A. Hannan, P. J. Ker, A. Hussain, M. B. Mansor, and F. Blaabjerg, "Review of energy storage system technologies in microgrid applications: Issues and challenges," *IEEE Access*, vol. 6, pp. 35 143–35 164, 2018.

[10] A. Tah and D. Das, "An enhanced droop control method for accurate load sharing and voltage improvement of isolated and interconnected dc microgrids," *IEEE Transactions on Sustainable Energy*, vol. 7, no. 3, pp. 1194–1204, 2016.

[11] T. Dragicevic, X. Lu, J. C. Vasquez, and J. M. Guerrero, "Dc microgrids - part i: A review of control strategies and stabilization techniques," *IEEE Transactions on Power Electronics*, vol. 31, no. 7, pp. 4876–4891, 2016.

[12] H. Wang, M. Han, R. Han, J. M. Guerrero, and J. C. Vasquez, "A decentralized current-sharing controller endows fast transient response to parallel dc–dc converters," *IEEE Transactions on Power Electronics*, vol. 33, no. 5, pp. 4362–4372, 2018.

[13] L. Meng, T. Dragicevic, J. C. Vasquez, and J. M. Guerrero, "Tertiary and secondary control levels for efficiency optimization and system damping in droop controlled dc-dc converters," *IEEE Transactions on Smart Grid*, vol. 6, no. 6, pp. 2615–2626, 2015.

[14] X. Lu, J. M. Guerrero, K. Sun, and J. C. Vasquez, "An improved droop control method for dc microgrids based on low bandwidth communication with dc bus voltage restoration and enhanced current sharing accuracy," *IEEE Transactions on Power Electronics*, vol. 29, no. 4, pp. 1800–1812, 2014.

[15] Q. Zhang, Y. Zeng, Y. Liu, X. Zhuang, H. Zhang, W. Hu, and H. Guo, "An improved distributed cooperative control strategy for multiple energy storages parallel in islanded dc microgrid," *IEEE Journal of Emerging and Selected Topics in Power Electronics*, vol. 10, no. 1, pp. 455–468, 2022.

[16] L. Xing, Y. Mishra, F. Guo, P. Lin, Y. Yang, G. Ledwich, and Y. C. Tian, "Distributed secondary control for current sharing and voltage restoration in dc microgrid," *IEEE Transactions on Smart Grid*, vol. 11, no. 3, pp. 2487–2497, 2020.

[17] W. Wu, Y. Chen, A. Luo, L. Zhou, X. Zhou, L. Yang, Y. Dong, and J. M. Guerrero, "A virtual inertia control strategy for dc microgrids analogized with virtual synchronous machines," *IEEE Transactions on Industrial Electronics*, vol. 64, no. 7, pp. 6005–6016, 2017.

[18] Z. Zhang, J. Fang, C. Dong, C. Jin, and Y. Tang, "Enhanced grid frequency and dc-link voltage regulation in hybrid ac/dc microgrids through bidirectional virtual inertia support," *IEEE Transactions on Industrial Electronics*, pp. 1–10, 2022.

[19] Y. Shan, J. Hu, K. W. Chan, Q. Fu, and J. M. Guerrero, "Model predictive control of bidirectional dc-dc converters and ac/dc interlinking converters-a new control method for pv-wind-battery microgrids," *IEEE Transactions on Sustainable Energy*, vol. 10, no. 4, pp. 1823–1833, 2019.

[20] P. Garcia-Trivino, J. P. Torreglosa, L. M. Fernandez-Ramirez, and F. Jurado, "Decentralized fuzzy logic control of microgrid for electric vehicle charging station," *IEEE Journal of Emerging and Selected Topics in Power Electronics*, vol. 6, no. 2, pp. 726–737, 2018.

[21] A. N. Akpolat, M. R. Habibi, E. Dursun, A. E. Kuzucuoglu, Y. Yang, T. Dragicevic, and F. Blaabjerg, "Sensorless control of dc microgrid based on artificial intelligence," *IEEE Transactions on Energy Conversion*, vol. 36, no. 3, pp. 2319–2329, 2021.
[22] N. H. Van Der Blij, L. M. Ramirez-Elizondo, M. T. J. Spaan, and P. Bauer, "Stability and decentralized control of plug-and-play dc distribution grids," *IEEE Access*, vol. 6, pp. 63 726–63 736, 2018.
[23] M. S. Sadabadi, Q. Shafiee, and A. Karimi, "Plug-and-play robust voltage control of dc microgrids," *IEEE Transactions on Smart Grid*, vol. 9, no. 6, pp. 6886–6896, 2018.
[24] D. Li and C. N. M. Ho, "A module-based plug-n-play dc microgrid with fully decentralized control for ieee empower a billion lives competition," *IEEE Transactions on Power Electronics*, vol. 36, no. 2, pp. 1764–1776, 2021.
[25] ——, "Decentralized pv-bes coordination control with improved dynamic performance for islanded plug-n-play dc microgrid," *IEEE Journal of Emerging and Selected Topics in Power Electronics*, vol. 9, no. 4, pp. 4992–5001, 2021.
[26] A. Q. Huang, M. L. Crow, G. T. Heydt, J. P. Zheng, and S. J. Dale, "The future renewable electric energy delivery and management (freedm) system: The energy internet," *Proceedings of the IEEE*, vol. 99, no. 1, pp. 133–148, 2011.
[27] J. Dugan, S. Mohagheghi, and B. Kroposki, "Application of mobile energy storage for enhancing power grid resilience: a review," *Energies*, vol. 14, no. 20, 2021.
[28] S. Lei, J. Wang, C. Chen, and Y. Hou, "Mobile emergency generator pre-positioning and real-time allocation for resilient response to natural disasters," *IEEE Transactions on Smart Grid*, vol. 9, no. 3, pp. 2030–2041, 2018.
[29] L. Che and M. Shahidehpour, "Adaptive formation of microgrids with mobile emergency resources for critical service restoration in extreme conditions," *IEEE Transactions on Power Systems*, vol. 34, no. 1, pp. 742–753, 2019.
[30] J. Su, K. Li, L. Zhang, X. Pan, and J. Yu, "A decentralized power allocation strategy for dynamically forming multiple hybrid energy storage systems aided with power buffer," *IEEE Transactions on Sustainable Energy*, pp. 1–11, 2023.
[31] Y. Xia, M. Yu, P. Yang, Y. Peng, and W. Wei, "Generation-storage coordination for islanded dc microgrids dominated by pv generators," *IEEE Transactions on Energy Conversion*, vol. 34, no. 1, pp. 130–138, 2019.
[32] J. Hu, Y. Shan, J. M. Guerrero, A. Ioinovici, K. W. Chan, and J. Rodriguez, "Model predictive control of microgrids – an overview," *Renewable and Sustainable Energy Reviews*, vol. 136, 2021.
[33] V. Nasirian, S. Moayedi, A. Davoudi, and F. L. Lewis, "Distributed cooperative control of dc microgrids," *IEEE Transactions on Power Electronics*, vol. 30, no. 4, pp. 2288–2303, 2015.
[34] S. Roberts, *DC/DC BOOK OF KNOWLEDGE*, 2015.
[35] TexasInstruments, "Basic calculation of a buck converter's power stage," Report, 2015.
[36] S. Bacha, I. Munteanu, and A. I. Bratcu, "Power electronic converters modeling and control," vol. 454, no. 454, 2014.
[37] P. Karamanakos, T. Geyer, N. Oikonomou, F. D. Kieferndorf, and S. Manias, "Direct model predictive control: A review of strategies that achieve long prediction intervals for power electronics," *IEEE Industrial Electronics Magazine*, vol. 8, no. 1, pp. 32–43, 2014.

Jialei Su was born in Shandong, China, in 1995. He received B.Eng. degree and M.Eng. degree in Electrical Engineering from Shandong University, Jinan, China, in 2017 and 2020, respectively.

He is currently persuing Ph.D. degree at the Electronic and Electrical Engineering from University of Leeds, United Kingdom. His research interests include DC microgrids control, battery energy storage management.

Kang Li (M'05–SM'11) received the B.Sc. degree in Industrial Automation from Xiangtan University, Hunan, China, in 1989, the M.Sc. degree in Control Theory and Applications from Harbin Institute of Technology, Harbin, China, in 1992, and the Ph.D. degree in Control Theory and Applications from Shanghai Jiaotong University, Shanghai, China, in 1995. He also received D.Sc. degree in Engineering from Queen's University Belfast, UK, in 2015.

Between 1995 and 2002, he worked at Shanghai Jiaotong University, Delft University of Technology and Queen's University Belfast as a research fellow. Between 2002 and 2018, he was a Lecturer (2002), a Senior Lecturer (2007), a Reader (2009) and a Chair Professor (2011) with the School of Electronics, Electrical Engineering and Computer Science, Queen's University Belfast, Belfast, U.K. He currently holds the Chair of Smart Energy Systems and leads the Institute of Communication and Power Networks at School of Electronic and Electrical Engineering, the University of Leeds, UK. His research interests cover nonlinear system modelling, identification, and control, and machine learning, with substantial applications to energy and power systems, smart grid, transport decarbonization, and energy management in energy intensive manufacturing processes. He has authored/co-authored over 200 journal publications and edited/co-edited 18 conference proceedings, winning over 20 prizes and awards.

Dr Li was the Chair of the IEEE UKRI Control and Communication Ireland chapter, the Secretary of the IEEE UK & Ireland Section. He is also a visiting professor of Shanghai Jiaotong University, Southeast University, Tianjin University, Shanghai University and Xiangtan University.

Chen Xing was born in Jinan, China, in 1994. He received the B.S. degree in automation from Hefei University of Technology, and the M.S. degree in control science and engineering from Shanghai University. He is currently pursuing the Ph.D. degree from the School of Electronic and Electrical Engineering, University of Leeds. His research interests include microgrid modelling, control and railway energy system optimization.